

High order predictor-corrector algorithms for strongly nonlinear problems

N. Kessab

Laboratoire de Calcul Scientifique en Mécanique, Faculté des Sciences Ben M'Sik,
Université Hassan II - Mohammadia, B.P. 7955, Sidi Othman, Casablanca, Maroc

B. Braikat

Laboratoire de Calcul Scientifique en Mécanique, Faculté des Sciences Ben M'Sik,
Université Hassan II - Mohammadia, B.P. 7955, Sidi Othman, Casablanca, Maroc

H. Lahmam

Laboratoire de Calcul Scientifique en Mécanique, Faculté des Sciences Ben M'Sik,
Université Hassan II - Mohammadia, B.P. 7955, Sidi Othman, Casablanca, Maroc

E. Mallil

Ecole Nationale Supérieure d'Electricité et de Mécanique,
Université Hassan II – Ain Chock, Casablanca, Maroc

N. Damil

Laboratoire de Calcul Scientifique en Mécanique, Faculté des Sciences Ben M'Sik,
Université Hassan II - Mohammadia, B.P. 7955, Sidi Othman, Casablanca, Maroc

M. Potier-Ferry

Laboratoire de Physique et Mécanique des Matériaux, UMR CNRS,
Université Paul Verlaine, Ile du Saulcy Metz, France

Abstract

We propose high order predictor-corrector algorithms to solve strongly non linear problems within the framework of the Asymptotic Numerical Method (ANM). The ANM associates asymptotic expansions with the Finite Element Method. We present a new predictor based on the concept of partial linearization (we keep only few non-linear terms). Three corrector algorithms will be tested in this paper: the well known Newton algorithm, a high order iterative Newton algorithm and a new high order algorithm that follows from the concept of partial linearization.

Résumé

Nous proposons un algorithme de prédiction correction d'ordre élevé, basé sur la méthode Asymptotique Numérique (MAN), pour résoudre des problèmes fortement non linéaires. La MAN associe les développements asymptotiques à la méthode des éléments finis. Nous présentons un nouveau prédicteur basé sur le concept d'une linéarisation partielle (nous gardons seulement peu de termes non linéaires). Trois algorithmes de corrections seront proposés dans cet article: l'algorithme connu de Newton, un algorithme itératif de type Newton d'ordre élevé et un nouvel algorithme d'ordre élevé basé sur une linéarisation partielle.

1. INTRODUCTION

We are interested by the numerical analysis of some non linear physical problems, where the main part of the nonlinearity of the response takes its origin from a small region. Let us consider for example unilateral contact problems. Sometimes, they are a few points, which transit between states with contact to state without contact. This generates a nonlinearity of the global response of the system. In deformation theory of plasticity, this can be the same for the points, which transit from the elastic to the plastic state.

In this paper, we limit ourselves to the response of plastic structures [6], [16], [18]. A typical stress-strain law is given on the figure1 (example of an elastoplastic law). One can distinguish three regions on this constitutive law: the region AB which corresponds to a linear law, the region CD which corresponds to a nearly linear law and the region BC which corresponds to a strongly nonlinear law. In the following, we shall try to develop predictor-corrector algorithms with a special treatment of this strongly nonlinear zone.

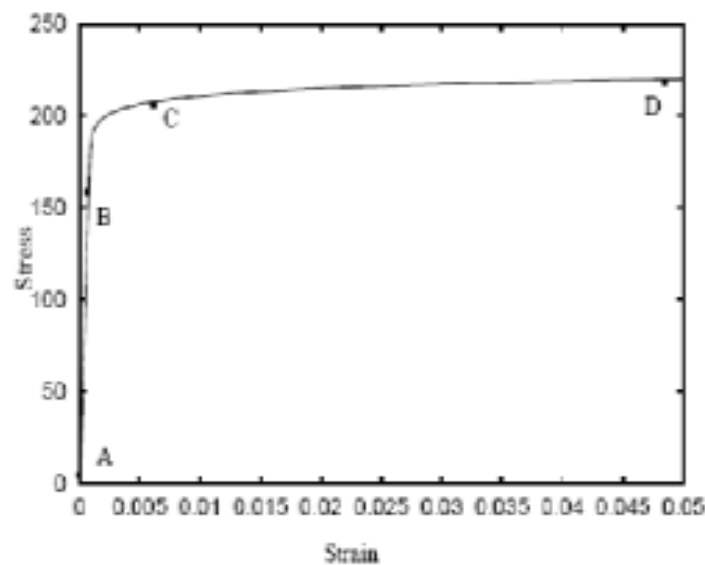


Figure 1: Constitutive law (deformation theory of plasticity)

In this paper, we shall introduce some new high order algorithms, within the framework of the Asymptotic Numerical Method (ANM). This numerical method associates asymptotic expansions [19], [24], [26], [14], [25], [29] with the finite element method [28] as presented in [8]. The unknowns of the nonlinear problem are expanded into series with respect to a "path" parameter and they are truncated at a high order. This procedure can be applied in a step by step manner, the end of the step being defined by a simple a posteriori analysis of series [7]. Recently, a more efficient algorithm has been introduced, that is based on Padé approximants [13]. These continuation algorithms are very efficient and robust, because no expensive correction phases are needed; the step lengths are large and adaptive. This has been successfully applied to strongly nonlinear problems [21], especially for plastic solids [4], [27]. We refer for instance to [12], [13], [22], [27] for a detailed bibliography. Nevertheless, we shall see that the absence of corrections leads to some computational difficulties within nearly perfect plasticity. That is why; we shall introduce predictor-corrector algorithms for a strongly nonlinear problem. The correctors are based on the coupling of a homotopy technique [2], [10] with the Asymptotic Numerical Method. Such high order iterative algorithms have been discussed [11], [17].

In this paper, we present a new predictor based on the concept of partial linearization: this means that we keep only few nonlinear terms, that correspond to a strongly nonlinear zone as the arc BC in figure 1. Several correctors will be discussed, especially a new one that follows from the principle of partial linearization.

This article is organized as follows: in Part 2, we review the Asymptotic Numerical Method in the case of the deformation theory of plasticity. Its cost and the reliability will be discussed and compared with classical techniques. We present the high order predictor in Part 3 and high order correctors in Part 4. The coupling of these techniques will be tested in Part 5 and evaluated by comparison to Newton-Raphson method [9], [23] and ANM.

2. THE ASYMPTOTIC NUMERICAL METHOD: A PATH FOLLOWING TECHNIQUE WITHOUT CORRECTOR

2.1 The test model: the deformation theory of plasticity

We consider the deformation theory of plasticity with a constitutive law based on the Ramberg-Osgood relationship. Consider a three dimensional plastic problem with a geometrical nonlinearity. The equilibrium equation can be written, in the reference domain Ω , as follows:

$$\langle \mathbf{R}(\mathbf{U}, \lambda), \delta \mathbf{u} \rangle = \int_{\Omega} {}^t \mathbf{S} : \delta \boldsymbol{\gamma}(\mathbf{u}) d\Omega - \lambda \int_{\partial \Omega} \mathbf{t} \delta \mathbf{u} ds = 0 \quad (1)$$

where $\mathbf{R}(\mathbf{U}, \lambda)$ is the global residual vector, \mathbf{S} is the second Piola-Kirchhoff stress tensor, λ is the loading parameter. The last term represents the work of external loads applied on the boundary $\partial \Omega$ and $\boldsymbol{\gamma}$ is the Green-Lagrange strain tensor, which is defined by:

$$\boldsymbol{\gamma}(\mathbf{u}) = \boldsymbol{\gamma}^l(\mathbf{u}) + \boldsymbol{\gamma}^{nl}(\mathbf{u}, \mathbf{u}) = \frac{1}{2}(\nabla \mathbf{u} + {}^t \nabla \mathbf{u}) + \frac{1}{2}({}^t \nabla \mathbf{u} \nabla \mathbf{u})$$

where u is the displacement vector. The Ramberg-Osgood relationship [1], [6] is given by:

$$E \boldsymbol{\gamma} = (1 + \nu) \mathbf{S}^d - (1 - 2\nu) P \mathbf{I} + \frac{3}{2} \alpha \left[\frac{S_{eq}}{\sigma_y} \right]^{n-1} \mathbf{S}^d \quad (2)$$

where E , ν , α , n and σ_y denote the Young's modulus, the Poisson's ratio, the yield offset, the hardening exponent and the yield stress respectively $P = -\frac{1}{3} \mathbf{S} : \mathbf{I}$ is the equivalent hydrostatic stress, $S_{eq} = \sqrt{\frac{3}{2} \mathbf{S}^d : \mathbf{S}^d}$ is the Mises equivalent stress, $\mathbf{S}^d = \mathbf{S} + P \mathbf{I}$ is the stress deviator tensor and \mathbf{I} is the identity tensor.

As the hardening exponent n is not necessary an integer, this law is not analytical for vanishing stress. That is why; the relationship (2) has to be regularized in order to apply expansions into power series. For this purpose, we can redefine the Mises equivalent stress in the following form:

$$\mathbf{S}_{\text{eq}}^2 = \frac{3}{2} \mathbf{S}^d : \mathbf{S}^d + \eta^2 \sigma_y^2 \quad (3)$$

where η denotes a regularization parameter. To obtain a quadratic framework, we introduce the following variables $\chi = \frac{\mathbf{S}_{\text{eq}}}{\sigma_y}$ and $\xi = \frac{3}{2} \alpha \chi^{n-1}$ and we transform the power law into a differential equation [21], [27]:

$$\chi d\xi = (n-1)\xi d\chi \quad (4)$$

Moreover, to keep the same initial slope as for non-regularized law, the left hand-side of equation (2) is multiplied by $(1 + \alpha \eta^n)$. The global structural problem is then formulated by the following equations which represent both equilibrium, constitutive relation and the two additional equations relative to the variables ξ and χ :

$$\left\{ \begin{array}{l} \int_{\Omega} \mathbf{S} : \delta \gamma(\mathbf{u}) d\Omega = \lambda \int \mathbf{t} \delta \mathbf{u} ds \\ \mathbf{E} (1 + \alpha \eta^n) \boldsymbol{\gamma} = (1 + \nu) \mathbf{S}^d - (1 - 2\nu) \mathbf{p} \mathbf{I} + \xi \mathbf{S}^d \\ \chi^2 = \frac{3}{2 \sigma_y^2} \mathbf{S}^d : \mathbf{S}^d + \eta^2 \\ \chi d\xi = (n-1)\xi d\chi \end{array} \right. \quad (5)$$

Alternative constitutive laws and regularization procedures should be treated in a similar way, see for instance [4], [27].

2.2 A review of the Asymptotic Numerical Method (ANM)

To solve the nonlinear problem (5) by the ANM, we expand the loading parameter λ and the mixed vector $\mathbf{U} = (\mathbf{u}, \mathbf{S}, \chi, \xi)$ into power series truncated at order N with respect to a path parameter "a". We seek a part of the solution branch in the neighbourhood of a known solution $(\mathbf{U}_0, \lambda_0)$ in the following form:

$$\left\{ \begin{array}{l} \mathbf{U}(\mathbf{a}) = \mathbf{U}_0 + \mathbf{a} \mathbf{U}_1 + \mathbf{a}^2 \mathbf{U}_2 + \dots + \mathbf{a}^p \mathbf{U}_p + \dots + \mathbf{a}^N \mathbf{U}_N \\ \lambda(\mathbf{a}) = \lambda_0 + \mathbf{a} \lambda_1 + \mathbf{a}^2 \lambda_2 + \dots + \mathbf{a}^p \lambda_p + \dots + \mathbf{a}^N \lambda_N \end{array} \right. \quad (6)$$

The path parameter is similar to the control parameter of classical iterative methods and it is defined by:

$$\mathbf{a} = \langle \mathbf{u} - \mathbf{u}_0, \mathbf{u}_1 \rangle + (\lambda - \lambda_0) \lambda_1 \quad (7)$$

where $\langle \cdot, \cdot \rangle$ is a scalar product. We substitute the expansions (6) into equilibrium and constitutive equations (5). Then, by equating like powers of "a", we obtain a sequence of N linear problems given, at each order p ($1 \leq p \leq N$), by:

$$\left\{ \begin{aligned} \int_{\Omega} \left\{ {}^t S_p : (\gamma^l(\delta u) + 2\gamma^{nl}(u_0, \delta u)) + {}^t S_0 : (\gamma^l(u_p) + 2\gamma^{nl}(u_0, u_p)) \right\} d\Omega &= \lambda_p \int_{\tilde{\alpha}\Omega} t \delta u ds - \int_{\Omega} \sum_{r=1}^{p-1} {}^t S_r : 2\gamma^{nl}(u_{p-r}, \delta u) d\Omega \\ S_p &= D_t : \left\{ \gamma^l(u_p) + 2\gamma^{nl}(u_0, u_p) + \sum_{r=1}^{p-1} \gamma^{nl}(u_r, u_{p-r}) \right\} + S_p^{res} \\ \chi_p &= \frac{3}{4\chi_0 \sigma_y^2} \sum_{i=0}^p S_i^d : S_{p-i}^d - \frac{1}{2\chi_0} \sum_{i=1}^{p-1} \chi_i \chi_{p-i} \\ \xi_p &= \frac{k}{p\chi_0} \sum_{i=1}^p i \chi_i \xi_{p-i} - \frac{1}{p\chi_0} \sum_{i=1}^{p-1} i \chi_{p-i} \xi_i \end{aligned} \right. \quad (8)$$

where D_t is the tangent modulus (see appendix A) and

$$S_p^{res} = -\frac{1}{E(1 + \alpha n^n)} D_t : \left\{ \sum_{i=1}^{p-1} \left(\xi_{p-i} S_i^d + \frac{3\xi_0(n-1)}{4\chi_0^2 \sigma_y^2} S_i^d : S_{p-i}^d - \frac{\xi_0(n-1)}{2\chi_0^2} \chi_i \chi_{p-i} + \frac{i}{p\chi_0} \left((n-1) \chi_i \xi_{p-i} - \chi_{p-i} \xi_i \right) \right) S_0^d \right\} \quad (9)$$

The linear equations (8) are condensed to drop S_p , χ_p , ξ_p and discretized by Finite Element Method. This yields equations in the following form:

$$\left\{ \begin{aligned} [K_t] \{u_p\} &= \lambda_p \{F\} + \{F_p^{nl}\} \\ {}^t \{u_p\} \{u_i\} + \lambda_p \lambda_i &= 0 \end{aligned} \right. \quad (10)$$

where $[K_t]$ denotes the tangent stiffness matrix computed at the initial solution U_0 and $\{u_p\}$ is the unknown nodal displacement vector at order p . Note that the stiffness matrix is the same for all the orders. The vector $\{F_p^{nl}\}$ depends on the previous orders.

The representation by series (6), truncated at order N , can be strongly improved by replacing the polynomial (6) by rational fractions $P_N(a)$ [3], [20]. The procedure is exactly the same as in [13] and it will be not repeated here. Roughly, it permits to reduce by half the number of steps.

A key point is the step end criterion, that permits to define a continuation procedure, see [7] for the case of a polynomial representation and [13] for the case of a rational representation. The principle of continuation consists to reapply the previous algorithm step by step to obtain the entire branch of the solution. In the case of a polynomial representation, the step end criterion corresponds to a maximum value a_m of the path parameter "a" given by the simple following relation:

$$a_m = \left(\delta \frac{\|\{u_i\}\|}{\|\{u_N\}\|} \right)^{\frac{1}{N-1}} \quad (11)$$

This value a_m depends on the choice of the small parameter δ , that is generally in the range from 10^{-3} to 10^{-8} . In the case of a rational representation, a very simple criterion is to require that the relative difference between two solutions at consecutive orders remains small. This can be expressed as (δ_1 being a small parameter):

$$\frac{\| \{P_N(a_{mp})\} - \{P_{N-1}(a_{mp})\} \|}{\| \{P_N(a_{mp})\} - \{u_0\} \|} < \delta_1 \quad (12)$$

These criteria (11) and (12) have the advantage to be clear and simple to be handled. Once the parameter δ or δ_1 has been chosen, the formula (11) or (12) defines an automatic and adaptive step length. In the practice, one chooses this parameter in order to get a wished accuracy at the end of the computation process, for instance in terms of a maximal residual κ :

$$\|R(U, \lambda)\| \leq \kappa \quad (13)$$

We shall see that the choice of δ is not so obvious for nearly perfect plasticity. The introduction of correction phases in the procedure will suppress the difficulty of an ad hoc choice of δ or δ_1 .

2.3 The test problem: bending of a plate

In order to discuss the performance of the proposed high order algorithms, we shall compare solutions obtained by ANM series, ANM Padé approximants and the classical Newton-Raphson algorithm [9], [23]. To this purpose, we consider the example of bending of a plate with length $L = 200 \text{ mm}$, width $l = 4 \text{ mm}$ and thickness $h = 1 \text{ mm}$. The material data are given as follows: $E = 2.10^5 \text{ MPa}$, $\nu = 0.3$, $\sigma_y = 200 \text{ MPa}$, $\alpha = 1$, $\varepsilon = 0.1$ and $n = 5$ or 40 . The plate is loaded by distributed homogeneous forces and discretized into 72 triangular elements with three nodes and two degrees of freedom per node see figure 2.

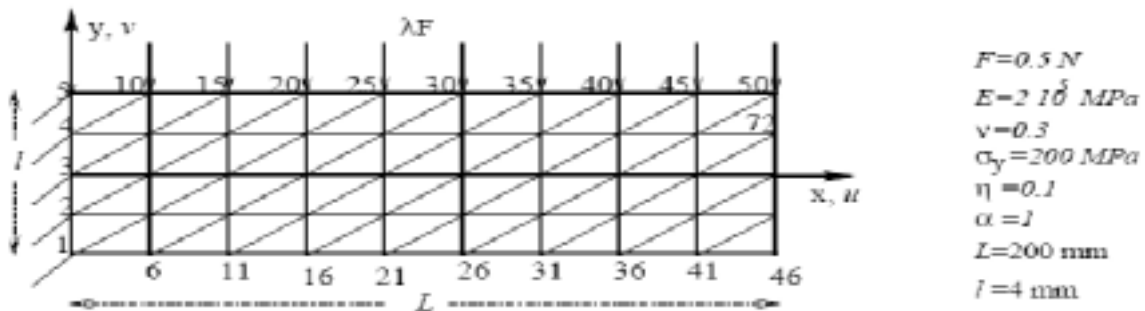


Figure 2: Clamped-free plastic plate under bending load λF

The aim is to search the response curve of vertical displacement v , at node 10, until $v = 2 \text{ mm}$ by varying the load λ . This curve will be searched with a $\kappa = 10^{-6}$, see (13). In this test, the geometrical nonlinearity has little influence, in which case the solution is probably unique for every value of λ . In such a case, an iterative method as the Newton-Raphson one is reliable and efficient. The numerical difficulties in this test come from the brutal change of the slope in the constitutive law in the

neighbourhood of the elastic limit. These difficulties are as much bigger than the hardening exponent n is large.

We shall test the case $n = 40$ for which the law is quasi-perfectly plastic. Traditionally, the difficulty of iterative predictor-corrector algorithms is the choice of the step length. In particular, it is necessary that the step length must be small so that there are sufficiently solution points to define the entire response curve. We didn't meet any particular difficulties to get the convergence of the Newton-Raphson algorithm. In the case of an exponent $n = 5$, we present the characteristics of two computations in table 1. One (with $\Delta l = 10$) gives a satisfactory number of points to describe all the curve (14 points), the other (with $\Delta l = 15$) provides only 9 points, what one can consider again as satisfactory (see figure 3-a). One can see that Newton Raphson algorithm needs an important number of matrix inversions to achieve the computations (table 1) (61 or 46 according to the number of wished points). In the case $n = 40$, three computations by Newton-Raphson algorithm are presented in table 2. For the two first of them ($\Delta l = 1, 3$), the number of steps and of iterations and hence of matrix inversions becomes more important: at least 129 inversions are needed. One can decrease this number of inversions ($\Delta l = 7$) but the number of solutions 8 points (12) becomes insufficient, especially as none of these points is located on the strongly nonlinear part (see figure 4-a). These first tests confirm the main quality of this algorithm that is its reliability, but also its large cost in terms of CPU time. Another difficulty is to choose the step Δl a priori.

Algorithm	Steps	Iterations	Inversions	Criterion
ANM series 19	17	0	17	$\delta=10^{11}$
ANM Padé 19	9	0	9	$\delta=10^{11}, \delta_1=10^{13}$
NR algorithm $\Delta\lambda=10$	14	47	61	$\kappa=10^6$
NR algorithm $\Delta\lambda=15$	9	39	46	$\kappa=10^6$

Table 1: Number of steps to go over from $\nu = 0$ to $\nu = 2$ mm. Algorithms ANM series order 19, ANM Padé order 19 and NR algorithm $n = 5$

Algorithm	Steps	Iterations	Inversions	Criterion
ANM series 19	71	0	71	$\delta=10^{19}$
ANM Padé 19	32	0	32	$\delta=10^{19}, \delta_1=10^{15}$
NR algorithm $\Delta\lambda=1$	95	203	298	$\kappa=10^6$
NR algorithm $\Delta\lambda=3$	32	97	129	$\kappa=10^6$
NR algorithm $\Delta\lambda=7$	(12)	(42)	(54)	$\kappa=10^6$

Table 2: Number of steps to go over from $\nu = 0$ to $\nu = 2$ mm. Algorithms ANM series order 19, ANM Padé order 19 and NR algorithm $n = 40$

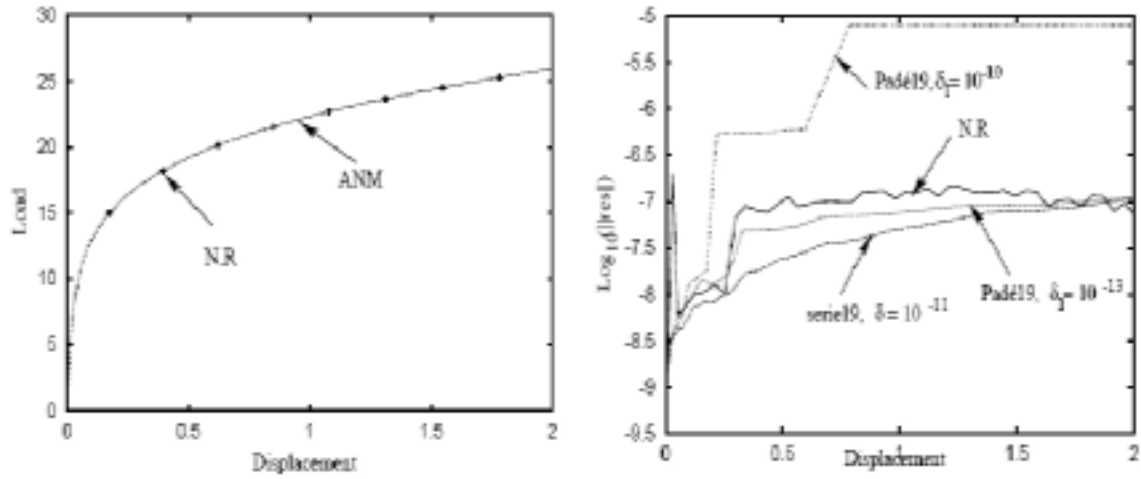


Figure 3: Load-displacement curve at node 10. Residual norm for NR, ANM series and ANM Padé order 19. $n = 5$

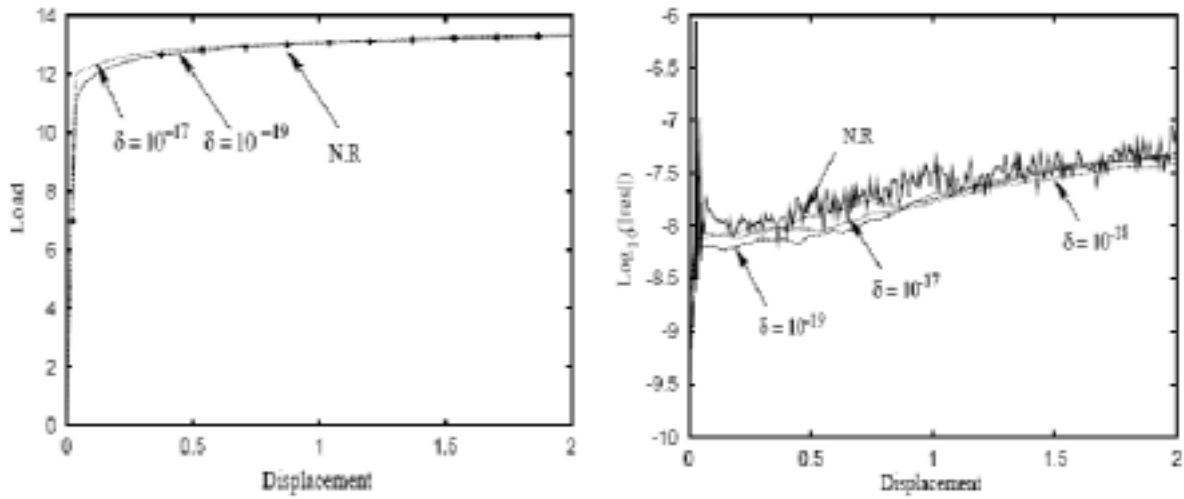


Figure 4: Load-displacement curve at node 10 and the residual norm for $n = 40$. Comparison between ANM series order 19 and Newton Raphson solutions for various values of δ

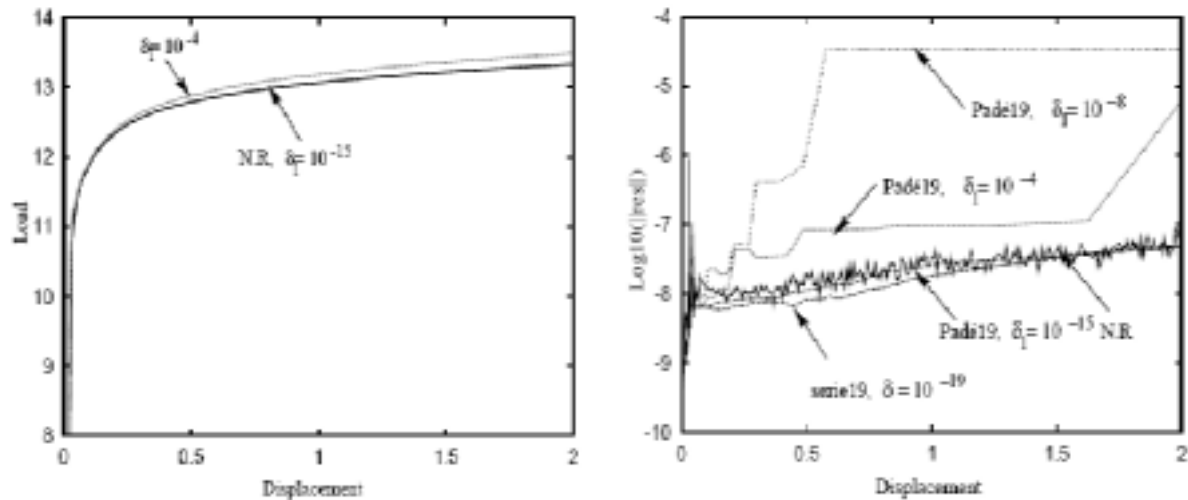


Figure 5: Load-displacement curve at node 10 and the residual norm for $n = 40$. Comparison between ANM Padé order 19 and Newton Raphson solutions for various values of δ_1 , $\delta = 10^{-19}$

On the contrary, the ANM defines a very efficient algorithm with a few number of computation steps. In addition, the step length is defined a posteriori, which suppress the difficulty due to the control of the algorithm. Nevertheless, the residual has tendency to increase during the step [7]. To this end, we must limit the step size in order to keep an acceptable residual by choosing an ad hoc control parameter δ or δ_1 . In the case $n = 5$, (see figure 3-b), one can see that these parameters must be chosen much smaller than in others cases previously studied. Another difficulty appears in the case $n = 40$. Indeed, the obtained response curve is not exact even for extremely small control parameters ($\delta = 10^{-17}$), although the residual is admissible (less than 10^{-6}) figure 4-b. This is due to ill conditioning of the compliance tangent matrix, that is to say that a strain increment modifies strongly the stress because of this nearly perfectly plastic law. It is therefore necessary to introduce correction phases in the ANM to circumvent these difficulties that not appear in the Newton-Raphson algorithm. On the other hand, when one finds a suitable control parameter δ , ANM is must faster than iterative algorithms. Indeed, the algorithm based on Padé approximants requires four or five times less matrix inversions than the Newton-Raphson method (see figure 5).

n	40	35.5	20	5
δ	10^{-19}	10^{-15}	10^{-10}	10^{-11}
δ_1	10^{-15}	10^{-12}	10^{-10}	10^{-13}
ANM series 19	71	40	20	17
ANM Padé 19	32	18	13	9
NR algorithm	129 ($\Delta\lambda=3$)	106 ($\Delta\lambda=3.4$)	87 ($\Delta\lambda=4.5$)	61 ($\Delta\lambda=10$)

Table 3: Number of matrix triangulations for ANM series order 19, ANM Padé order 19 and N.R algorithm versus the hardening exponent n . Note that the ad hoc choice of δ and δ_1 is not so obvious. Several step lengths have been tested with NR and we have presented the fastest one

One can also verify that the introduction of rational fractions reduces by half the number of steps for an equivalent cost, as in many previous tests. The results with others values of the hardening exponent

are given in table 3: one can see that the adjustment of the controlling parameters δ and δ_i is not easy in these examples. That is why we have introduced a correction phase in the ANM.

3. A HIGH ORDER PREDICTOR BASED ON THE CONCEPT OF PARTIAL LINEARIZATION

We present here new high order predictor-corrector algorithms, where the predictor and the correctors are computed from series and/or Padé approximants. The aim is to reconcile the robustness of an iterative algorithm as the Newton-Raphson method with the efficiency of ANM. Indeed, the interest of ANM is to give an excellent predictor that permits, in one hand, to perform great steps and therefore to reduce strongly the computation time, on the other hand to define a posteriori the step length that becomes also naturally adaptive. The introduction of correction phases at the step end should permit to increase the robustness of the ANM algorithms and to reduce the difficulty that is due to the choice of controlling parameters δ and δ_i .

High order corrector algorithms have been introduced recently [11], [17] by coupling a homotopy transformation with a perturbation technique. The most natural idea is to concatenate a prediction given by the formula (15) with these high order correctors. This discussion has been realized in a parallel work [15].

We present here a little more complex algorithm that accounts for the local character of the strong nonlinearity. The most original aspect is the predictor that is based on the concept of partial linearization. The idea is to replace the nonlinear system (5) by a partially linearized problem where only the most significant nonlinear terms are kept. This system will be solved step by step with one correction at step end. Finally, this system will be redefined when the corrector algorithm doesn't converge or not enough quickly. In other words, we introduce two concepts of steps. First of all, we define great steps in the following way: we restart with a new great step when one redefines the nonlinear system characterising the predictor. Inside a given great step, there may be several small steps that are nothing but the steps of solving the partially linearized system. A correction phase is performed at the end of each small step. The global sketch of the algorithm is presented in figure 8. In this part, we limit ourselves to the definition of the predictor that holds good for one great step and hopefully several small steps.

Stage 1: Definition of a strongly non-linear zone

The first stage consists in defining a strongly non-linear zone at a given starting solution point (U_0, λ_0) of the problem (5). One defines as follows the strongly non-linear zone that will be called *zone II* (see figure 1). A point of the structure will be considered in the strongly non-linear *zone II* if the ratio of Mises stress on the yield stress verifies the following condition:

$$a < \frac{S_{eq}}{\sigma} < b \quad (14)$$

where a and b are two real numbers to be chosen. The complementary part of the zone II is called zone I. In what follows, a tangent stiffness matrix $[K_{II}]$ will be associated with this zone II and the global matrix $[K]$ will be solved by a block decomposition. In order that this solving procedure is efficient, we limit the size of the zone II to about 30% of the whole structure. If the size of this zone II goes beyond this limit, we propose to forsake the procedure of partial linearization and to compute the next step by another technique. Here, we shall use the ANM Padé to carry out the computation of the latter

steps. In the same way, we use this ANM procedure without correction if no points lie in the zone II. In other words, the following procedure of partial linearization is used only if the number of points in the zone II is strictly positive, but lowers than a limit of about 30%.

$$0 \% < \text{percentage zone II} < 30\% \tag{15}$$

Stage 2: definition of the partially linearized problem

This stage consists in introducing a partial linearization of the problem (5) around the starting point (U_0, λ_0) . One defines incremental unknowns $U = U_0 + \Delta U$ and $\lambda = \lambda_0 + \Delta \lambda$. The Green- Lagrange strain tensor is then rewritten as:

$$\gamma(u) = \gamma(u_0) + \gamma^L(u_0, \Delta u) + \gamma^{nl}(\Delta u, \Delta u)$$

with

$$\gamma^L(u_0, \Delta u) = \gamma^l(\Delta u) + \frac{1}{2}({}^t\nabla\Delta u\nabla u_0 + {}^t\nabla u_0\nabla\Delta u)$$

By injecting these new variables in the problem (5), one gets the following nonlinear problem satisfied by the new unknowns $\Delta U, \Delta \lambda$:

$$\left\{ \begin{array}{l} \int_{\Omega} ({}^t\Delta S : \gamma^L(u_0, \delta u) + 2S_0 : \gamma^{nl}(\Delta u, \delta u) + 2\Delta S : \gamma^{nl}(\Delta u, \delta u))d\Omega = \Delta \lambda \int_{\tilde{\Omega}} t\delta u ds \\ E(1 + \alpha\eta^n) \left(\gamma^L(u_0, \Delta u) + \gamma^{nl}(\Delta u, \Delta u) \right) = (1 + \nu)\Delta S^d - (-2\nu)\lambda PI + \xi_0\Delta S^d + \Delta\xi(S_0^d + \Delta S^d) \\ \Delta\chi^2 + 2\chi_0\Delta\chi = \frac{3}{2\sigma_y^2} (S_0^d : \Delta S^d + \Delta S^d : S_0^d + \Delta S^d : \Delta S^d) \\ (\chi_0 + \Delta\chi)d\Delta\xi = (n-1)\xi_0 + \Delta\xi \end{array} \right. \tag{16}$$

We approximate the problem (16) in the following manner. First, we linearize the first equation (equilibrium) all over the domain Ω . Second, we linearize the second equation (constitutive law) only in *zone I* and we keep the exact constitutive law in the strongly non-linear *zone II*. The geometrical non-linearity is considered as smooth, so the non-linear term in the left hand-side of (16-b) is dropped. Thus the partially linearized problem is then defined by:

$$\left\{ \begin{array}{l} \int_{\Omega} ({}^t\Delta S : \gamma^L(u_0, \delta u) + 2S_0 : \gamma^{nl}(\Delta u, \delta u))d\Omega = \Delta \lambda \int_{\tilde{\Omega}} t\delta u ds \\ \gamma^L(u_0, \delta u) = (M + H_0) : \Delta S \quad \text{in I} \\ E(1 + \alpha\eta^n) \gamma^L(u_0, \Delta u) = (1 + \nu)\Delta S^d - (-2\nu)\lambda PI + \xi_0\Delta S^d + \Delta\xi(S_0^d + \Delta S^d) \quad \text{in II} \\ \Delta\chi^2 + 2\chi_0\Delta\chi = \frac{3}{2\sigma_y^2} (S_0^d : \Delta S^d + \Delta S^d : S_0^d + \Delta S^d : \Delta S^d) \\ (\chi_0 + \Delta\chi)d\Delta\xi = (n-1)\xi_0 + \Delta\xi \end{array} \right. \tag{17}$$

Where $(M+H_0)^{-1}$ is the tangent stiffness tensor calculated at the starting point U_0 . This simplified non-linear problem will be solved in a step-by-step method: in the following, these steps will be designated as small steps. After this simplification, the local stiffness matrices in *zone I* depend only on U_0 and not on ΔU : this means that we shall keep the same stiffness matrix in the *zone II* for all these small steps. This simplification is the main interest of the partial linearization technique

Stage 3: solution of the partially linearized problem

To solve the non-linear problem (17), we shall apply the ANM (see section 2.1). So, the solution ΔU , $\Delta \lambda$ are searched in the form (N_p is the order of the predictor):

$$\begin{cases} \Delta U(\mathbf{a}) = \Delta U_0 + \mathbf{a} \Delta U_1 + \mathbf{a}^2 \Delta U_2 + \dots + \mathbf{a}^{N_p} \Delta U_{N_p} \\ \Delta \lambda(\mathbf{a}) = \Delta \lambda_0 + \mathbf{a} \Delta \lambda_1 + \mathbf{a}^2 \Delta \lambda_2 + \dots + \mathbf{a}^{N_p} \Delta \lambda_{N_p} \end{cases} \quad (18)$$

$$\mathbf{a} = \frac{1}{\Delta L^2} \left\{ \langle \Delta \mathbf{u} - \Delta \mathbf{u}_0, \Delta \mathbf{u}_1 \rangle + (\Delta \lambda - \Delta \lambda_0) \Delta \lambda_1 \right\} \quad (19)$$

where $\Delta \lambda$ is the equivalent of the arc length parameter. The procedure of expansions into series is the same as in several previous papers [4], [8], [13], [27] and the details are reported in the appendix A.

Stage 4: discretization and condensation

In this stage, we transform the linear problem by discretization and condensation. We distinguish, at each order p , the degrees of freedom of the *zone I* and *zone II*. The obtained linear problems (29) (see appendix A) can be written in the following form:

$$\begin{bmatrix} [K_I] & [K_c] \\ [K_c] & [K_{II}] \end{bmatrix} \begin{Bmatrix} \Delta U_p^I \\ \Delta u_p^{II} \end{Bmatrix} = \Delta \lambda_p \begin{Bmatrix} \mathbf{f}^I \\ \mathbf{f}^{II} \end{Bmatrix} + \begin{Bmatrix} \mathbf{0} \\ \mathbf{F}_p^{nl} \end{Bmatrix} \quad (20)$$

where $[K_I]$ denotes a tangent stiffness matrix for the *zone I* that depend only on the starting point U_0 . This is the same for the couplage matrix $[K_c]$. $[K_{II}]$ is the tangent stiffness matrix of *zone II*. $\{\Delta u_p^I\}$ and $\{\Delta u_p^{II}\}$ are respectively the degrees of freedom of the *zone I* and *zone II*. $\{\mathbf{f}^I\}$ and $\{\mathbf{f}^{II}\}$ are known load vectors. $\{\mathbf{F}_p^{nl}\}$ is a vector that contains non-linear terms including displacement and stress field computed at previous orders (lower than p). Because $[K_I]$ and $[K_c]$ do not change during a great step it is interesting to solve (20) by a block decomposition technique. Thus we can eliminate the degrees of freedom $\{\Delta u_p^I\}$ as follows:

$$\{\Delta u_p^I\} = -[K_I]^{-1} [K_c] \{\Delta u_p^{II}\} + \Delta \lambda_p [k_I]^{-1} \{\mathbf{f}^I\}$$

So, the problem (20) can be transformed in the following form:

$$[k_{II}^*] \{\Delta u_p^{II}\} = \Delta \lambda_p \{\mathbf{f}^{II*}\} + \{\mathbf{F}_p^{nlII}\} \quad (21)$$

where $[k_{II}^*]$ and $\{\mathbf{f}^{II*}\}$ are given by:

$$[k_{II}^*] = [k_{II}]^{-1} [k_c] [k_I]^{-1} [k_c] \tag{22}$$

$$\{f^{II*}\} = \{f^{II}\}^{-1} [k_c] [k_I]^{-1} \{f^I\}$$

Note that we do not invert the global stiffness matrix in this procedure. Let us recall that this algorithm is well adapted only if the size of the matrix $[K_{II}]$ is small. The computation time in this procedure is mainly due

- first, to the triangulation of the great matrix $[K_I]$;
- second, to the products of matrices in the second term of the right hand-side in (22);
- last, to the triangulation of the small matrices $[K_{II}^*]$; this has to be done at the beginning of each small step.

It is not obvious that the previous procedure is always the best possible one. Especially, this can depend on the relative size of the *zone II*. Indeed, the condensed matrix $[K_{II}^*]$ is not as sparse as the initial matrix $[K_I]$ and the time needed for its triangulation can be too large. That is why we can consider either to invert directly the system (20) at each small step or to solve (21) by an iterative technique as the conjugated gradient [5].

Examples

We consider the example of subsection 2.2. For a first analysis of the so defined prediction, we perform a few steps with the ANM Padé, in the same way as in Part 2, up to the first appearance of points in the *zone II*. Next, we present the prediction branches obtained by solving the problem (17), by the step by step procedure described previously for several values of the interval $[a, b]$ and for $n = 5, 40$. The accuracy parameter to define the end of a small step is $\delta = 10^{-8}$. The obtained results are presented in table 4 and in figures 6, 7. Several values of the interval $[a, b]$ are considered to define the strongly non-linear zone. In figure 6, we present some prediction branches obtained by solving problem (17) for different values of $[a, b]$ with ANM series truncated at *order 20*. As expected, the definition of the interval $[a, b]$ has an influence on the starting point of the procedure and on the size of the strongly non-linear zone. A larger values of the parameter a delays the beginning of the procedure. The number of points in the *zone II* remains rather small, in the range 6% - 18%. On the figures 6, 7, one sees that the response curves move away from the reference. Apparently, the best prediction is obtained for $[a, b] = [0.8, 1.2]$ and $[0.9, 1.1]$ in the case $n = 40$, and for another interval $[a, b] = [0.95, 1.]$ in the case $n = 5$. Nevertheless, we shall see that the appearance of the prediction curves is not a measure of its capacity to furnish good prediction points. The values of the residual do not yield such a criterion: indeed the residual is generally larger than 10^{-2} , but this doesn't prevent the convergence of various iterative algorithms.

n	[0.8, 1.2]		[0.9, 1.1]		[0.95, 1.0]	
	v_0	% zone II	v_0	% zone II	v_0	% zone II
5	0.0418	18	0.0585	18	0.1175	6
40	0.0264	16	0.0269	6	0.0365	18

Table 4: Characteristics of the starting point of the procedure of partial linearization. v_0 is the initial deflexion at node 10. The size of the matrix $[K_{II}]$ follows from the percentage of nodal points in the strongly non-linear *zone II*

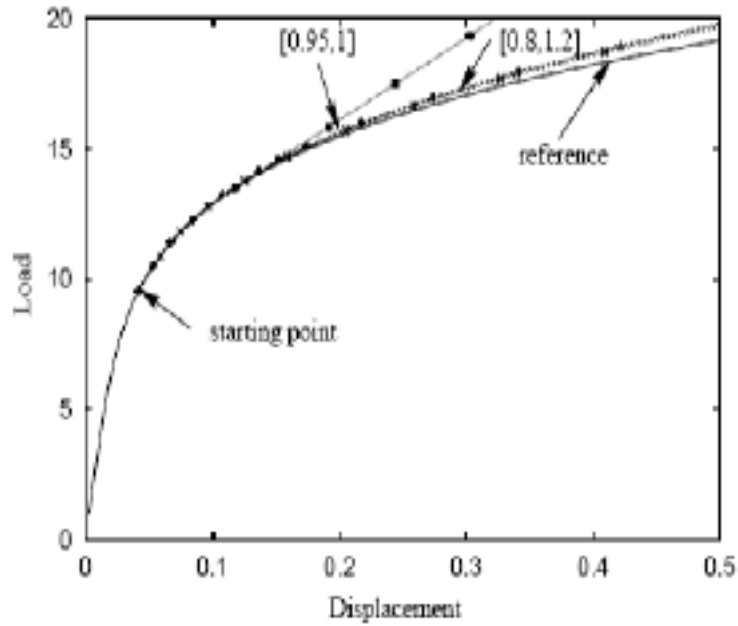


Figure 6: Load-displacement curve at node 10 and prediction branch's obtained by ANM series truncated at order 20 for $n=5$ for different intervals $[a, b]$

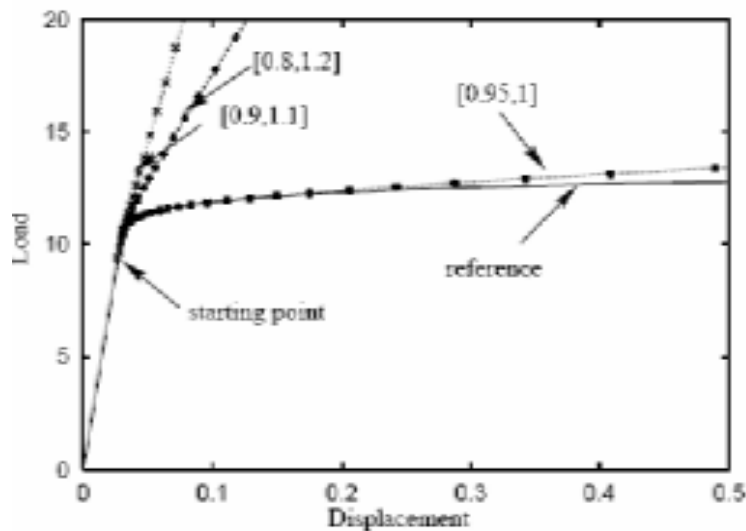


Figure 7: Load-displacement curve at node 10 and prediction branch's obtained by ANM series truncated at order 20 for $n=40$ for different intervals $[a, b]$

4. HIGH ORDER CORRECTORS

Three corrector algorithms will be tested in this paper: the well known Newton algorithm, a high order iterative Newton algorithm that has been introduced recently [11], [17] and at last a new high order algorithm that is also based on the concept of partial linearization. The two first ones have the drawback to require one triangulation of a great matrix per iteration. The new algorithm is based on the concept of homotopy transformation [2], [10]. In [11], [17], such transformations have been introduced, not only to define high order Newton iterations, but also to introduce continuous transformation from an arbitrary system to the system to be solved. Here, the arbitrary system is linear,

the matrix being exactly the same as in the predictor. In this section, we suppose known a prediction point (U^p, λ^p) . We shall present these three corrector algorithms to get a good approximation of a solution close to this prediction point.

4.1 Newton correctors

In this paper, we shall test first the concatenation of the predictor of partial linearization with the classical first order Newton algorithm. For completeness, the formulae for the increments are recalled in Appendix B. Note that the tangent operator is exactly the same as with ANM, see Part 2. Generally, the convergence is achieved after several iterations and therefore after several triangulations of tangent matrices. Likely, the modified Newton algorithm does not converge very well for a strongly nonlinear problem as the one studied here.

Next, the predictor will be associated with the high order Newton algorithm. The principle is to define a homotopy transformation from a linear system into the system to be solved. In this case, the linear system is exactly the one of the first Newton correction. The modified system is then solved by a perturbation technique, the homotopy parameter ε being the expansion parameter. The convergence of the series is accelerated by introducing Padé approximants. The formulae to compute the series are detailed in Appendix B.

4.2 A high order corrector based on the concept of partial linearization

In the previous section, we have presented a high order predictor and we have obtained some prediction branches. On these prediction branches, we consider some prediction points (U^p, λ^p) that will be corrected by a high order corrector. The main idea of this corrector is to apply a homotopy technique, which consists to search the solution of the exact problem (5) in the form:

$$(U, \lambda) = (U_0, \lambda_0) + (\Delta U(\varepsilon), \Delta \lambda(\varepsilon))$$

where ε is the homotopy parameter and $\Delta U = (\Delta u(\varepsilon), \Delta S(\varepsilon), \Delta \chi(\varepsilon), \Delta \xi(\varepsilon))$. The vector $(\Delta U(\varepsilon), \Delta \lambda(\varepsilon))$ satisfies the following problem:

$$\left\{ \begin{array}{l} \int_{\Omega} ({}^t \Delta S : \gamma^L(u_0, \delta u) + 2S_0 : \gamma^{nl}(\Delta u, \delta u) + 2\varepsilon \Delta S : \gamma^{nl}(\Delta u, \delta u)) d\Omega = \Delta \lambda \int_{\tilde{\Omega}} t \delta u ds \\ \gamma^L(u_0, \Delta u) + \varepsilon \gamma^{nl}(\Delta u, \Delta u) = (M + H_0) \Delta S + \varepsilon \left(\frac{1}{E(1 + \alpha \eta^p)} (\xi_0 \Delta S^d + \Delta \xi (S_0^d + \Delta S^d)) - H_0 \Delta S \right) \quad \text{in I} \\ E(1 + \alpha \eta^p) (\gamma^L(u_0, \Delta u) + \varepsilon \gamma^{nl}(\Delta u, \Delta u)) = (1 + \nu) \Delta S^d - (1 - 2\nu) \Delta \Pi I + \xi_0 \Delta S^d + \Delta \xi (S_0^d + \Delta S^d) \quad \text{in II} \\ \Delta \chi^2 + 2\chi_0 \Delta \chi = \frac{3}{2\sigma_y^2} (S_0^d : \Delta S^d + \Delta S^d : S_0^d + \Delta S^d : \Delta S^d) \\ (\chi_0 + \Delta \chi) d\Delta \xi = (n - 1) (\xi_0 + \Delta \xi) d\Delta \chi \end{array} \right. \quad (23)$$

By this way, the vector $(\Delta U(\varepsilon), \Delta \lambda(\varepsilon))$, that is solution of the correction problem (23), passes continuously from the solution of the partially linearized problem (16) for $\varepsilon = 0$ to an exact solution of (5) for $\varepsilon = 1$. The correction problem (23) at $\varepsilon = 0$ involves in zone I, the tangent operator at the starting point U_0 of the great step and in zone II, the tangent operator at the prediction point $U_0 + \Delta U_0$. So, only a small part, $[K_{II}]$, of the tangent matrix changes along the great step. To solve the nonlinear

problem (23), we use the ANM algorithm based on Padé approximants. First, we search a parametric representation of the solution path $(\Delta U(\varepsilon), \Delta \lambda(\varepsilon))$ in the form of truncated integro-powers series with respect to the parameter ε (N_c is the order of the corrector).

$$\Delta U(\varepsilon) = \sum_{p=0}^{N_c} \varepsilon^p \Delta U_p \quad \Delta \lambda(\varepsilon) = \sum_{p=0}^{N_c} \varepsilon^p \Delta \lambda_p \quad (24)$$

Next, these series are replaced by Padé approximants using the same technique as previously. Another key point to establish this algorithm is the choice of the strategy to specify the variation of $\Delta \lambda$. As in the classical arc-length algorithms, the most natural way is to require the correction $(\Delta u - \Delta u_0, \Delta \lambda - \Delta \lambda_0)$ to be orthogonal to the slope of the response curve. This slope $(\Delta u', \Delta \lambda')$ is easily computed from the prediction branch since we have an analytic representation of this latter. This yields the following relation:

$$\langle \Delta u - \Delta u_0, \Delta u' \rangle + (\Delta \lambda - \Delta \lambda_0) \Delta \lambda' = 0 \quad (25)$$

One can find in the Appendix A the linear systems characterising each term $(\Delta U_p, \Delta \lambda_p)$ of the series (24).

After discretization and condensation like for the prediction, these linear problems can be written in a similar form as previously:

$$\begin{bmatrix} [K_I] & [K_c] \\ [K_c]^t & [K_{II}] \end{bmatrix} \begin{Bmatrix} \Delta u_p^I \\ \Delta u_p^{II} \end{Bmatrix} = \Delta \lambda_p \begin{Bmatrix} f^I \\ f^{II} \end{Bmatrix} + \begin{Bmatrix} F_p^{nII} \\ F_p^{nIII} \end{Bmatrix} \quad (26)$$

In this paper, the linear system (26) is solved by block decomposition: indeed only the small matrix $[K_{II}]$ differs from the tangent matrix at the starting point (U_0, λ_0) of the great step. According to the procedure of Part 3, the same global matrix is also used for the next prediction small step.

5. COUPLING THE PREDICTOR AND THE CORRECTORS

Now let us summarize the general sketch of the predictor-corrector algorithm. One original point is to distinguish two types of steps, (see figure 8). At the beginning of one great step, the tangent matrix is up-dated. Normally a great step includes several small steps and only a small part of the tangent matrix is up-dated at each small step. We have chosen two criterions to define automatically the end of these steps. First, the end of the small step is defined by the analysis of the series as within ANM. As for a great step, one continues it as long as the corrector converges. Note also that this predictor-corrector technique is used only when the strongly linear zone exists and its size is not too large. Otherwise, the current step is achieved by the ANM Padé method without correction.

5.1 Global sketch of the algorithm

- 1 Choose a starting point (here $(U_0=0, \lambda_0=0)$)
- 2 Define the strongly non-linear zone (*zone II*) and test its size by formulae (15)
 - 2-a If the test is satisfied, go to 4
 - 2-b If not, go to 3

- 3 One great step by ANM Padé
 - 3-a Compute the branch $(U(a), \lambda a)$ at order N_A by (8)
 - 3-b Define the end of the step according to (12) depending on the small parameter δ_1
 - 3-c Return to 2
- 4 One great step by partial linearization
 - 4-a Compute the prediction branch by solving (17) by ANM series at order N_p (small step)
 - 4-b Define the end of the small step by (11) depending on the small parameter δ
 - 4-c Correct this end point by one of the algorithms of Part 4
 - 4-d Check the convergence of the correctors
 - If convergence, return to 4-a (new small step)
 - If not, keep the latest corrected point and return to 2 (for a new great step)
- 5 Stop when the wished response curve has been computed

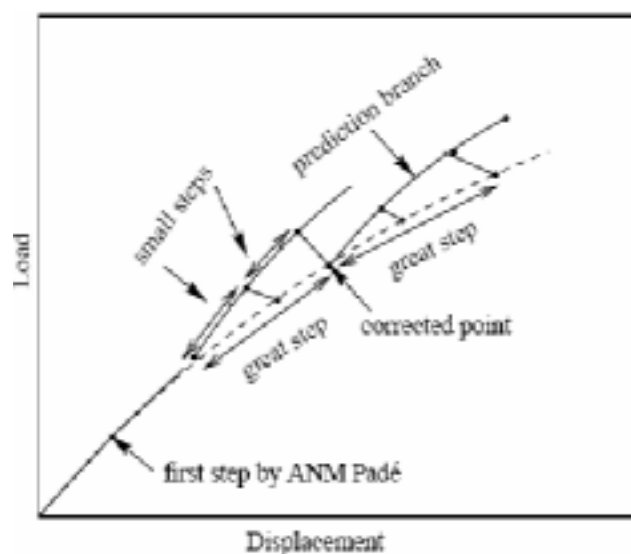


Figure 8: Global sketch of the algorithm: Great steps and small steps

With respect to others procedures, these algorithms would reduce the number of triangulations of great matrices. Indeed, one expects a limited number of great steps. In the case of the partial linearization corrector, one deals with only one great matrix $[K_I]$ per great step (and, of course, one great matrix $[K_I]$ per ANM step). In the case of (high order) Newton corrector, one adds one great matrix $[K_I]$ per iteration. Furthermore, one triangulates $(n_{ss}+2)$ small matrices $[K_{II}^*]$ if the great step includes n_{ss} small steps. As explained in section 3.4, the corresponding computing time is not negligible if the size of these matrices is too large.

5.2 Application

This algorithm will be now tested with the same example as in Part 2: bending of a plate, with a hardening exponent $n = 40$ or $n = 5$.

In the step 4-d of the algorithm (Part 5.1), we assume that the iteration process is convergent if

$$\|R(U, \lambda)\| \leq \kappa \quad (27)$$

and we keep $\kappa = 10^{-6}$ in the applications. If a step is computed by ANM Padé as in Part 2, we adjust the parameter δ_l in such a way that the residual remains within this limit: we have seen that one has to choose $\delta_l = 10^{-15}$ for $n = 40$ and $\delta_l = 10^{-13}$ for $n = 5$. The orders of expansions are chosen as: (N_A is the order of the great step by ANM Padé, N_p is the order of the predictor and N_c is the order of the corrector)

$$N_A=19, \quad N_p=N_c=20$$

The high order correctors will be limited to a single iteration. In the case of the Newton algorithm, several iterations are always necessary, and one decides that it diverges if the residual increases too much after 2 or 3 iterations.

5.3 Numerical results with partial linearization

5.3.1 Newton corrector, n=40

We shall first analyse the coupling of Newton corrector with the partial linearization predictor. We have always verified that the corrected points are on the reference curve and there is no deviation as observed on figure 4. A computation example is presented on the figure 9. In this figure, $[a, b]=[0.9, 1.1]$ and the algorithm uses 5 great steps by ANM Padé without correction and then 5 great 20 steps by the proposed algorithm. These 5 great steps include 12 small steps (see table 5). One can see on the figure 9 that these results permit to describe with a good accuracy the response curve until $v = 2 \text{ mm}$. In table 5, we report some characteristics of computation results: the number of ANM steps, the number of great and small steps, the number of iterations, the number of great and small matrices to triangulate and the mean size of small matrices $[K_{II}^*]$. This computation has been effected for different values of the interval $[a, b]$ that defines the *zone II*.

Algorithm		Number or nature of steps			Number or nature of steps	Small matrices	
ANM Padé		32			32		
Proposed algorithm	ANM step	Predictor-corrector			iteration	Number	Mean size
		Great steps	Small steps				
[0.95,1.]	9	5	13	54	(9+3x5+54) 78	14	16x16
[0.8,1.]	1	9	18	75	103	19	17x17
[0.9,1.1]	5	5	12	60	80	13	16x16
[0.8,1.2]	1	9	18	74	102	19	21x21

Table 5: Partial linearization predictor ($N_p = 20$) coupled with the Newton-corrector ($N_c = 1$) and comparison with ANM Padé ($N_A = 19$) in the case of $n=40$

The main result is the reduction of the number of great steps (10 to 14 including the ANM steps instead of 32 with the ANM Padé without correction). Indeed, the absence of correction obliged us to use smallest steps by a very small choice of δ and δ_1 . Here, the length of great steps follows particularly from the required accuracy $\kappa = 10^{-6}$. That is why; the step length is much larger than with ANM without correction. This effect is manifest on the figure 9: just before the *point A*, a very small length has been obtained during 4 steps when, just after this point, the change of the algorithm has much increased the size of steps. The cost of this algorithm is more important than the one of ANM Padé, because of a great number of matrix inversions in the correction phase (from 78 to 103). Nevertheless, the total number of a great matrix inversions remains in general smaller than the one of Newton algorithm (129, after several tests of arc-length (table 2)). The presence of correction permits to stabilize the ANM Padé algorithm. We see in the table 5 that the choice of the interval $[a, b]$ doesn't influence radically the computation cost. We have also verified that is the same for the parameter δ that controls the size of small steps. The very good results in term of great step length are also due to the quality of the partial linearization predictor. It remains to test the contribution of correctors that are less expansive in computation time.

5.3.2 High order corrector, n=40

We present the obtained results by replacing the corrector of *order I* by a Padé corrector of order $N_c=20$. The quality of the high order corrector has permitted to limit the algorithm to one iteration and therefore to a great matrix inversion per small step. The number of great matrix inversions is in the same range as the one within ANM Padé: from 35 to 41 instead of 32, see table 6. Therefore this algorithm has almost the same efficiency that the ANM Padé algorithm while keeping the robustness of the Newton algorithm. Indeed, the present algorithm is really appreciable that to the required accuracy κ .

Algorithm		Number or nature of steps		Number or nature of steps	Small matrices	
ANM Padé		32		32		
Proposed algorithm	ANM step	Predictor-corrector			Number	Mean size
		Great steps	Small steps + iteration			
[0.95,1.]	9	7	18	41 (9+2x7+18)	19	15x15
[0.8,1.]	1	8	21	38	22	20x20
[0.9,1.1]	5	8	16	37	17	19x19
[0.8,1.2]	1	7	20	35	21	24x24

Table 6: Partial linearization predictor ($N_p = 20$) coupled with the high order Newton-corrector ($N_c = 20$) and comparison with ANM Padé ($N_A = 19$) in the case of $n=40$

On the contrary, with the ANM without correction, one must adjust the parameters δ and δ_1 that is difficult in this example; in the same way with Newton-Raphson algorithm, one must fix the step length that has a great influence on the rapidity of the algorithm. Let us note also that the number of small steps and the size of the *zone II* remain reasonable, which permits to hope that the computation cost remains limited.

5.3.3 The partial linearization corrector, $n=40$

The coupling of the predictor and of the partial linearization corrector permits to reduce the number of great matrix to be inverted. Indeed, one can perform all the small steps inside a great step with only one great matrix inversion. We observe that the number of these inversions is always lower than 32, as required by the ANM (see table 7). The choice of the interval $[a, b]$ has an influence on the computation cost. It is necessary that the parameter 'a' of the interval $[a, b]$ must be at some distance from 1 ($a = 0.8$ or 0.9) to limit the number of steps without partial linearization (see table 7): one had seen that they were needlessly small (see figure 9). The best way is to take an interval centred around 1. For this test, the choice of the biggest interval $[0.8, 1.2]$ would be recommended because it doesn't increase meaningfully the size of small matrices $[K_{II}^*]$. Let's note that the number of great matrices can be reduced to 5 (table 7) (instead of 32 with ANM Padé and 129 with Newton-Raphson). The number of small matrices remains limited as in the best case, the total number of matrices (5 great + 29 small) remains nearly the same that with the ANM Padé algorithm.

Algorithm	Number or nature of steps		Number or nature of steps	Small matrices		
ANM Padé	32		32			
Proposed algorithm	ANM step	Predictor-corrector		Number	Mean size	
		Great steps	Small steps + iteration			
[0.95,1.]	14	11	14	25	36	13x13
[0.8,1.]	3	10	21	13	41	19x19
[0.9,1.1]	5	7	17	12	31	20x20
[0.8,1.2]	1	4	21	5	29	22x22

Table 7: Partial linearization predictor ($N_p = 20$) coupled with the partial linearization-corrector ($N_c = 20$) and comparison with ANM Padé ($N_A = 19$) in the case of $n=40$

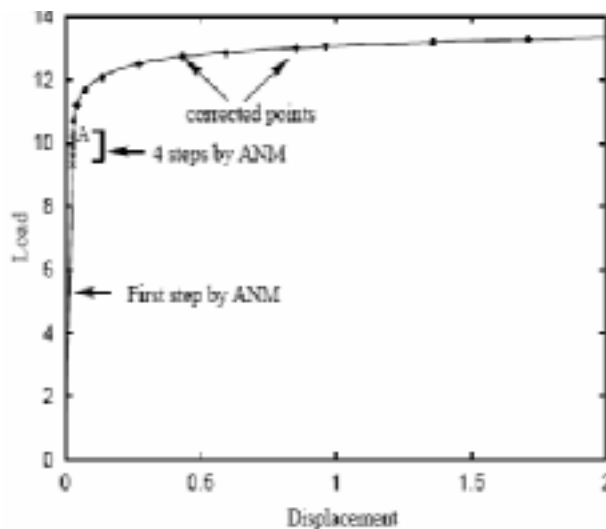


Figure 9: $n=40$: the predictor-corrector algorithm yields solutions points on the response curve. Here the five first steps have been computed by ANM Padé, that yields a continuous response curve OA. Main characteristics of the algorithm: Newton corrector, $a = 0.9$, $b = 1.1$, $N_p = 20$, $N_A = 19$, $\kappa = 10^{-6}$

5.3.4 The partial linearization corrector, $n=5$

Finally, we have tested these algorithms with others constitutive laws, i.e others exponents n . We limit ourselves here to the case $n=5$, where the constitutive law is more regular and where we can to ask if it is useful to distinguish a strong non-linear zone. We present only the results obtained by the partial linearization corrector.

The number of obtained great steps (ANM Padé and partial linearization predictor-corrector) is little less dependent on parameters of the algorithm (a , b , δ) and it remains in the same range as the one of the ANM without correction (8 to 10 instead of 9 see table 8). In this case, the most efficient algorithm is the one with a small interval $[a, b] = [0.95, 1]$: it seems that we could do without the partial linearization and that it was probably sufficient to associate a cheap corrector with the ANM Padé predictor.

Algorithm		Number or nature of steps		Number or nature of steps	Small matrices	
ANM Padé		9		9		
Proposed algorithm	ANM step	Predictor-corrector			Number	Mean size
		Great steps	Small steps + itération			
[0.95,1.]	5	3	3	8	9	10x10
[0.8,1.]	4	6	8	10	20	21x21
[0.9,1.1]	4	5	7	9	17	21x21
[0.8,1.2]	4	5	8	9	18	26x26

Table 8: Partial linearization predictor ($Np = 20$) coupled with the partial linearization-corrector ($Nc = 20$) and comparison with ANM Padé ($NA = 19$) in the case of $n=5$

6. CONCLUSION

In this article, we have introduced specific algorithms for problems having a very strong non-linearity localized in the spatial domain and in the constitutive law. These algorithms are within the framework of ANM methods because the predictor and correctors involve expansions into series and Padé approximants. We have only considered an example with few degrees of freedom in the case of a solid nearly elastic perfectly plastic. The results have been compared, in first, to Newton-Raphson method, and in second, to the ANM method without correction. Indeed, in this case, the first algorithm is robust, but requires many iterations. With the second, one must reduce, in a heuristic manner, the step length to avoid in a appearance of false solutions due to the ill-conditioning of the stiffness tangent matrix. On the contrary, the proposed algorithms are reliable and automatic. Indeed, we had not found false solutions and these algorithms doesn't require to fix a priori a step length or an adjustable parameter. In fact, they depend nearly only on the wanted accuracy and on the orders of truncature.

The most original point is the predictor that is non-linear. It is based on the concept of partial linearization that permits to limit the non-linearity to a few nodal points. Several correctors have been tested. According to our tests, the most efficient one is a new high order corrector that is also based on partial linearization. The coupling of the predictor and of the correctors can reduce significantly the number of triangulations of matrices with respect to ANM without corrector.

As compared to more classical predictor-correctors methods, the present algorithm has completely adaptive steps. This adaptivity is due, first to a posteriori analysis of series as within ANM, second to

an analysis of the convergence of the correctors. This algorithm is not completely optimized and it should be validated by more realistic structural computations. Especially, the inversion technique of the small matrices, the definition of the strongly non-linear zone should be rediscussed and possible correctors during the first steps should be introduced.

Independently of the partially linearization technique, the association of high order predictors and correctors leads to efficient and robust algorithms. We refer to a companion paper [15] for alternative validations of this idea.

REFERENCES

1. Abaqus. Theory and users' manuals (version 5.5), Hibbit, Karlsson and Sorenson, Inc., 1080 Main Street, Pawtucket, RI 02860, USA, (1995).
2. Allgower E. L. and Georg K., Numerical Continuation Methods. An Introduction, Springer Series in Computational Mathematics, 13, Springer-Verlag (1990).
3. Baker G. A. and Graves Morris P., Padé Approximants, Encyclopedia of Mathematics and its Applications, 13, n°1, (1981), Addison-Wesley Publishing Company, New York.
4. Braikat B., Damil N. and Potier-Ferry M., Méthodes Asymptotiques Numériques pour la plasticité. *Revue Européenne des Eléments Finis*, Hermès, Paris, 6 (3), 337-357 (1997).
5. Ciarlet P. G., Introduction à l'analyse numérique matricielle et à l'optimisation, Masson, (1980).
6. Chen W. F., Constitutive Equations for Engineering Materials, Elsevier, Plasticity and modelling 2 (1994).
7. Cochelin B., A path-following technique via an asymptotic-numerical method. *Computers and Structures* 53, 1181-1192 (1994).
8. Cochelin B., Damil N. and Potier-Ferry M., The asymptotic-numerical method: an efficient perturbation technique for non-linear structural mechanics. *Revue Européenne des Eléments Finis*, 3, 281--297 (1994).
9. Crisfield M. A., Non-linear finite element analysis of solids and structures, John Wiley & Sons, 2 (1997).
10. Dale-Martin E., A technique for accelerating iterative convergence in numerical integration with application in transonic aerodynamics. Springer-Verlag, H. Cabannes editor, Lectures Notes in Physics, 47, 123-139 (1976).
11. Damil N., Potier-Ferry M., Najah A., Chari R. and Lahmam H., An iterative method based upon Padé Approximants. *Communications in Numerical Methods in Engineering*, 15, 701-708 (1999).
12. Elhage Hussein A., Damil N. and Potier-Ferry M., An asymptotic numerical algorithm for frictionless contact problems. *Revue Européenne des Eléments Finis*, Hermès, Paris, 7 (3), 119-130 (1998).
13. Elhage Hussein A., Potier-Ferry M. and Damil N., A numerical continuation method based on Padé approximants. *International Journal of Solids and Structures*, 37, 6981-7001, (2000).
14. Kawahara M., Yoshimura N., Nakagawa K. and Ohsaka K., Steady and unsteady finite element analysis of incompressible viscous fluid. *International Journal of Numerical Methods in Engineering*, 10, 437-456, (1976).
15. Lahmam H., Cadou J. M., Zahrouni H., Damil N. and Potier-Ferry M., High order predictor-corrector algorithms, *International Journal of Numerical Methods in Engineering*, 55, 685-704, (2002).
16. Lemaitre J. and Chaboche J. L., *Mécanique des matériaux solides*, Dunod (1985).

17. Mallil E., Lahmam H., Damil N. and Potier-Ferry M., An iterative process based on homotopy and perturbation techniques. *Computer Methods in Applied Mechanics and Engineering*, Volume 190, Number 13, pp. 1845-1858(14), 22 December 2000
18. Maugin G. A., *The Thermomechanics of Plasticity and Fracture*, Cambridge University Press (1992).
19. Noor A. K. and Peters J. M., Tracing post-limit-point paths with reduced basis technique. *Computer Methods in Applied Mechanics and Engineering*, 28, 217-240 (1981).
20. Padé H., Sur la représentation approchée d'une fonction par des fractions rationnelles, *Annales de l'Ecole Normale Supérieure* (1892). 9(3), pp 3-93, 1892.
21. Potier-Ferry M., Damil N., Braikat B., Descamps J., Cadou J. M., Cao H. L. and Elhage Hussein A., Traitement des fortes non-linéarités par la méthode asymptotique numérique. *Compte Rendue de l'Académie des Sciences, Paris*, t.324, Série II b, {171-177 (1997)}.
22. Potier-Ferry M., Cao H. L., Descamps J. and Damil N., An asymptotic numerical method for numerical analysis of large deformation viscoplastic problems., unpublished
23. Riks E., Some computational aspects of the stability analysis of nonlinear structures. *Computer Methods in Applied Mechanics and Engineering* 47, 219-259 (1984).
24. Thompson J. M. T. and Walker A. C., The non-linear perturbation analysis of discrete structural systems. *International Journal of Solids and Structures*, 4,757-768 (1968).
25. Van-Dyke M., Computed-extended series. *Annual Review in Fluid Mechanics*, 16, 287-309 (1984).
26. Yokoo Y., Nakamurat T. and Ueteni K., The incremental perturbation method for large displacement analysis of elastic-plastic structures. *International Journal of Numerical Method in Engineering*, 10, 503-525 (1976).
27. Zahrouni H., Potier-Ferry M., Elasmr H. and Damil N., Asymptotic numerical method for nonlinear constitutive laws. *Revue Européenne des Eléments Finis*, Hermès, Paris, 7, 841-869 (1998).
28. Zienkiewicz O. C. and Taylor R. L., *The Finite Element Method*. McGraw-Hill Book Company, 4th edn (1991).
29. Méthodes asymptotiques numériques, *Revue européenne des éléments finis* Vol 13 – n 1-2, 2004.

Appendix A: Resolution of the prediction and correction problems by ANM

A.1: Resolution of the prediction problem by ANM

By substituting (18) into (17) and (19), we obtain a sequence of linear problems satisfied by the terms $(\Delta U_i, \Delta \lambda_i)$ that we can write in the following form:
order l

$$\left\{ \begin{aligned} & \int_{\Omega} \Delta S_1 : \gamma^L(u_0, \delta u) + 2S_0 : \gamma^{nl}(\Delta u_1, \delta u) d\Omega = \Delta \lambda_1 \int_{\partial\Omega} t \delta u ds \\ & \gamma^L(u_0, \Delta u_1) = (M + H_0) : \Delta S_1 \quad \text{in } I \\ & E(1 + \alpha \eta^n) \gamma^L(u_0, \Delta u_1) = (1 + \nu) \Delta S_1^d - (1 - 2\nu) \Delta P_1 I + (\Delta \xi_0 + \xi_0) \Delta S_1^d + \Delta \xi_1 (S_0^d + \Delta S_0^d) \quad \text{in } II \\ & 2(\Delta \chi_0 + \chi_0) \Delta \chi_1 = \frac{3}{2\sigma_y^2} \left((S_0^d + \Delta S_0^d) : \Delta S_1^d + \Delta S_1^d : S_0^d + \Delta S_1^d : \Delta S_0^d \right) \\ & (\Delta \chi_0 + \chi_0) \Delta \xi_1 = (n-1) (\Delta \xi_0 + \xi_0) \Delta \chi_1 \\ & \langle \Delta u_1, \Delta u_1 \rangle + \Delta \lambda_1 \Delta \lambda_1 = \Delta L^2 \end{aligned} \right. \quad (28)$$

order $p > 1$

$$\left\{ \begin{aligned} & \int_{\Omega} \Delta S_p : \gamma^L(u_0, \delta u) + 2S_0 : \gamma^{nl}(\Delta u_p, \delta u) d\Omega = \Delta \lambda_p \int_{\partial\Omega} t \delta u ds \\ & \gamma^L(u_0, \Delta u_p) = (M + H_0) : \Delta S_p \quad \text{in } I \\ & E(1 + \alpha \eta^n) \gamma^L(u_0, \Delta u_p) = (1 + \nu) \Delta S_p^d - (1 - 2\nu) \Delta P_p I \\ & \quad + (\Delta \xi_0 + \xi_0) \Delta S_p^d + \Delta \xi_p (S_0^d + \Delta S_0^d) + \sum_{i=1}^{p-1} \Delta \xi_i \Delta S_{p-i}^d \quad \text{in } II \\ & 2(\Delta \chi_0 + \chi_0) \Delta \chi_p + \sum_{i=1}^{p-1} \Delta \chi_i \Delta \chi_{p-i} = \frac{3}{2\sigma_y^2} \left(2(S_0^d + \Delta S_0^d) : \Delta S_p^d + \sum_{i=1}^{p-1} \Delta S_i^d \Delta S_{p-i}^d \right) \\ & p(\Delta \chi_0 + \chi_0) \Delta \xi_p + \sum_{i=1}^{p-1} i \Delta \chi_i \Delta \xi_{p-i} = (n-1) \left(p (\Delta \xi_0 + \xi_0) \Delta \chi_p + \sum_{i=1}^{p-1} i \Delta \chi_{p-i} \Delta \xi_i \right) \\ & \langle \Delta u_p, \Delta u_1 \rangle + \Delta \lambda_p \Delta \lambda_1 = 0 \end{aligned} \right. \quad (29)$$

These problems involve many variables. By substituting the laws according to zones I and II, we obtain an equilibrium relation where the displacement field Δu_p at order p is the principal unknown:

$$\left\{ \begin{aligned} & \int_{\Omega} \gamma^L(u_0, \delta u) : D_I : \gamma^L(u_0, \Delta u_p) + 2S_0 : \gamma^{nl}(\Delta u_p, \delta u) d\Omega = \Delta \lambda_p \int_{\partial\Omega} t \delta u ds \quad \text{in } I \\ & \int_{\Omega} \gamma^L(u_0, \delta u) : D_{II} : \gamma^L(u_0, \Delta u_p) + 2S_0 : \gamma^{nl}(\Delta u_p, \delta u) d\Omega = \Delta \lambda_p \int_{\partial\Omega} t \delta u ds \\ & \quad + \frac{1}{E(1 + \alpha \eta^n)} \int_{\Omega} \gamma_p^{res} : D_{II} : \gamma^L(u_0, \delta u_p) d\Omega \quad \text{in } II \\ & \langle \Delta u_p, \Delta u_1 \rangle + \Delta \lambda_p \Delta \lambda_1 = 0 \end{aligned} \right. \quad (30)$$

Where γ_p^{res} is a residual strain that depends on orders less than p . It is given by:

$$\begin{aligned} \gamma_p^{res} = & \sum_{i=1}^{p-1} \Delta \xi_{p-i} \Delta S_i^d + \sum_{i=1}^{p-1} \left[\frac{3(\xi_0 + \Delta \xi_0)(n-1)}{4(\chi_0 + \Delta \chi_0)^2 \sigma_0^2} \Delta S_i^d : \Delta S_{p-i}^d - \frac{(\xi_0 + \Delta \xi_0)(n-1)}{2(\chi_0 + \Delta \chi_0)^2} \Delta \chi_i \Delta \chi_{p-i} \right. \\ & \left. + \frac{i}{p(\chi_0 + \Delta \chi_0)} \left((n-1) \Delta \chi_i \Delta \xi_{p-i} - \Delta \chi_{p-i} \Delta \xi_i \right) \right] (\Delta S_0^d + S_0^d) \end{aligned} \quad (31)$$

and D_I, D_{II} are the tangent modulus for zone I and zone II respectively.

$$D_t = E \left\{ \left(1 + \nu + \xi_0 \right) I_1 - \left(\nu + \frac{\xi_0}{3} \right) I_2 + k_1 \Sigma \right\}^{-1}$$

With $k_1 = \frac{3(n-1)\xi_0}{2\chi_0\sigma_y^2}$ $[I_2] = \begin{pmatrix} 1 & 1 & 0 \\ 1 & 1 & 0 \\ 0 & 0 & 0 \end{pmatrix}$ $[I_1] = \begin{pmatrix} 1 & 0 & 0 \\ 0 & 1 & 0 \\ 0 & 0 & 2 \end{pmatrix}$

$$[\Sigma] = \begin{pmatrix} S_{0xx}^d S_{0xx}^d & S_{0xx}^d S_{0yy}^d & 2S_{0xx}^d S_{0xy}^d \\ S_{0yy}^d S_{0xx}^d & S_{0yy}^d S_{0yy}^d & 2S_{0yy}^d S_{0xy}^d \\ 2S_{0xy}^d S_{0xx}^d & 2S_{0xy}^d S_{0yy}^d & 4S_{0xy}^d S_{0xy}^d \end{pmatrix}$$

The tangent modulus D_t used in section 2 has the same expression as D_l , where (S_0, χ_0, ξ_0) is the initial point of the ANM step. D_{II} is the same as D_l , but we replace the initial point (S_0, χ_0, ξ_0) by $(S_0 + \Delta S_0, \chi_0 + \Delta \chi_0, \xi_0 + \Delta \xi_0)$

A.2: Resolution of the correction problem by ANM

Introducing (24) into (23) and (25), we obtain the following sequence of linear problems satisfied by the vector ΔU_p and the parameter $\Delta \lambda_p$ at a given order "p"

$$\left\{ \begin{aligned} & \int_{\Omega} \Delta S_p : \gamma^L(u_0, \delta u) + 2S_0 : \gamma^{nl}(\Delta u_p, \delta u) d\Omega = \Delta \lambda_p \int_{\Omega} t \delta u ds - 2 \int_{\Omega} \sum_{i=1}^{p-2} \Delta S_{p-i-1} : \gamma^{nl}(\Delta u_i, \delta u) d\Omega \\ & E(1 + \alpha \eta^n) \left(\gamma^L(u_0, \Delta u_p) + 2\gamma^{nl}(\Delta u_0, \Delta u_{p-1}) + \sum_{i=1}^{p-2} \gamma^{nl}(\Delta u_i, \Delta u_{p-i-1}) \right) = E(1 + \alpha \eta^n) \\ & ((M + H_0) : \Delta S_p - H_0 : \Delta S_{p-1}) + (\Delta \xi_0 + \xi_0) \Delta S_{p-1} + \Delta \xi_{p-1} (S_0^d + \Delta S_0^d) + \sum_{i=1}^{p-2} \Delta \xi_i \Delta S_{p-i-1} \quad in I \\ & E(1 + \alpha \eta^n) \left(\gamma^L(u_0, \Delta u_p) + 2\gamma^{nl}(\Delta u_0, \Delta u_{p-1}) + \sum_{i=1}^{p-2} \gamma^{nl}(\Delta u_i, \Delta u_{p-i-1}) \right) = (1 + \nu) \Delta S_p^d - (1 - 2\nu) \Delta P_p I \\ & \quad + (\Delta \xi_0 + \xi_0) \Delta S_p^d + \Delta \xi_p (S_0^d + \Delta S_0^d) + \sum_{i=1}^{p-1} \Delta \xi_i \Delta S_{p-i}^d \quad in II \\ & 2(\Delta \chi_0 + \chi_0) \Delta \chi_p + \sum_{i=1}^{p-1} \Delta \chi_i \Delta \chi_{p-i} = \frac{3}{2\sigma_y^2} \left(2(S_0^d + \Delta S_0^d) : \Delta S_p^d + \sum_{i=1}^{p-1} \Delta S_i^d \Delta S_{p-i}^d \right) \\ & p(\Delta \chi_0 + \chi_0) \Delta \xi_p + \sum_{i=1}^{p-1} i \Delta \chi_i \Delta \xi_{p-i} = (n-1) p (\Delta \xi_0 + \xi_0) \Delta \chi_p + \sum_{i=1}^{p-1} i \Delta \chi_{p-i} \Delta \xi_i \\ & \langle \Delta u_p, \Delta u \rangle + \Delta \lambda_p \Delta \lambda = 0 \end{aligned} \right. \tag{32}$$

Appendix B: Newton correctors

The problem to be solved is

$$\left\{ \begin{array}{l} \int_{\Omega} {}^t S : \delta \gamma(u) d\Omega = \lambda \int_{\partial\Omega} t \delta u ds \\ E(1 + \alpha \eta^n) \gamma = (1 + \nu) S^d - (1 - 2\nu) P I + \xi S^d \\ \chi^2 = \frac{3}{2\sigma_y^2} S^d : S^d + \eta^2 \\ \chi d\xi = (n-1) \xi d\chi \end{array} \right. \quad (33)$$

Let (U^1, λ^1) be a given trial solution of the problem (33). We try to define iteratively other approximated solutions (U^p, λ^p)

At the next iteration, $(p+1)$, the correction $(\Delta U = U^{p+1} - U^p, \Delta \lambda = \lambda^{p+1} - \lambda^p)$ should satisfy exactly the following equations:

$$\langle R_e^{p+1}, \delta u \rangle = \langle R(U^{p+1}, \lambda^{p+1}), \delta u \rangle = \int_{\Omega} \left(\Delta S : \gamma^L(u^p, \delta u) + S^p : 2\gamma^{nl}(\Delta u, \delta u) \right) d\Omega - \Delta \lambda \int_{\partial\Omega} t \delta u ds + \langle R_e^p, \delta u \rangle = 0 \quad (34)$$

$$\begin{aligned} R_e^{p+1} &= \gamma^L(u^p, \Delta u) + \gamma^{nl}(\Delta u, \Delta u) + R_e^p \\ &- \frac{1}{E(1 + \alpha \eta^n)} \left\{ (1 + \nu) \Delta S^d - (1 - 2\nu) \Delta P I + \xi^p \Delta S^d + \Delta \xi S^{pd} + \Delta \xi \Delta S^d \right\} = 0 \end{aligned} \quad (35)$$

Where R_e^p is the equilibrium residual vector, R_c^p is the constitutive law residual vector:

$$\langle R_e^p, \delta u \rangle = \langle R(U^p, \lambda^p), \delta u \rangle = \int_{\Omega} {}^t S^p : \gamma^L(u^p, \delta u) d\Omega - \lambda^p \int_{\partial\Omega} t \delta u ds \quad (36)$$

$$\begin{aligned} R_c^p &= \left(\gamma^L(u^p) + \gamma^{nl}(u^p, u^p) \right) \\ &- \frac{1}{E(1 + \alpha \eta^n)} \left\{ (1 + \nu) S^{pd} - (1 - 2\nu) P I - \xi^p S^{pd} \right\} \end{aligned} \quad (37)$$

B.1: Newton corrector

At iteration $p+1$, we solve the following problem

$$\left\{ \begin{array}{l} \int_{\Omega} \left({}^t \Delta S : \gamma^L(u^p, \delta u) + S^p : 2\gamma^{nl}(\Delta u, \delta u) \right) d\Omega + \langle R_e^p, \delta u \rangle - \Delta \lambda \int_{\partial\Omega} t \delta u ds = 0 \\ E(1 + \alpha \eta^n) \left(\gamma^L(u^p, \Delta u) + R_c^p \right) - (1 + \nu) \Delta S^d - \left((1 - 2\nu) \Delta P I + \xi^p \Delta S^d + \Delta \xi^p S^{pd} \right) = 0 \\ 2\chi^p \Delta \chi + 2\Delta \chi \Delta \chi - \frac{3}{2\sigma_y^2} \left(S^{pd} : \Delta S^d + \Delta S^d : S^{pd} + \Delta S^d : S^d \right) = 0 \\ (\chi^p + \Delta \chi) d\Delta \xi - (n-1) \xi^p d\Delta \chi - (n-1) \Delta \xi d\Delta \chi = 0 \end{array} \right. \quad (38)$$

B.2: High order corrector

At iteration $p+1$, we solve the following problem

$$\left\{ \begin{aligned} & \int_{\Omega} \left(\Delta S : \gamma^L(u^p, \delta u) + S^p : 2\gamma^{nl}(\Delta u, \delta u) + 2\Delta S : \gamma^{nl}(\Delta u, \delta u) \right) d\Omega + \varepsilon \langle R_c^p, \delta u \rangle - \Delta \lambda \int_{\tilde{\alpha}\Omega} t \delta u ds = 0 \\ & E(1 + \alpha \eta^n) \left(\gamma^L(u^p, \Delta u) + \gamma^{nl}(\Delta u, \Delta u) + \varepsilon R_c^p \right) \\ & - \left((1 + \nu) \Delta S^d - (1 - 2\nu) \Delta PI + \xi^p \Delta S^d + \Delta \xi (S^{pd} + \Delta S^d) \right) = 0 \\ & 2\chi^p \Delta \chi + \Delta \chi^2 - \frac{3}{2\sigma_y^2} (S^{pd} : \Delta S^d + \Delta S^d : S^{pd} + \Delta S^d : \Delta S^d) = 0 \\ & (\chi^p + \Delta \chi) d\Delta \xi = (n-1) (\xi^p + \Delta \xi) d\Delta \chi \end{aligned} \right. \quad (39)$$

We compute the solution by seeking $(\Delta U, \Delta \lambda)$ in the form of truncated series

$$\left\{ \begin{aligned} \Delta U(\varepsilon) &= \varepsilon \Delta U_1 + \varepsilon^2 \Delta U_2 + \dots + \varepsilon^r \Delta U_r + \dots + \varepsilon^N \Delta U_N \\ \Delta \lambda(\varepsilon) &= \varepsilon \Delta \lambda_1 + \varepsilon^2 \Delta \lambda_2 + \dots + \varepsilon^r \Delta \lambda_r + \dots + \varepsilon^N \Delta \lambda_N \end{aligned} \right. \quad (40)$$

This leads to solve N linear problems that can be written at each order r as follows:

$$\left\{ \begin{aligned} & \int_{\Omega} \left(\gamma^L(u^p, \Delta u_r) : D_t : \gamma^L(u^p, \delta u) + S^p : 2\gamma^{nl}(\Delta u_r, \delta u) \right) d\Omega = \Delta \lambda_r \int_{\tilde{\alpha}\Omega} t \delta u ds + \langle F_r^{nl}, \delta u \rangle \\ & \Delta S_r = D_t \left(\gamma^L(u^p, \Delta u_r) + \sum_{i=1}^{r-1} \gamma^{nl}(\Delta u_i, \Delta u_{r-i}) \right) + \Delta S_r^{res} \\ & \langle F_r^{nl}, \delta u \rangle = - \int_{\Omega} (\Delta S_r^{res} : \gamma^L(u^p, \delta u) + \sum_{i=1}^{r-1} \gamma^{nl}(\Delta u_i, \Delta u_{r-i}) : D_t : \gamma^L(u^p, \delta u) \\ & + \sum_{i=1}^{r-1} \Delta S_{r-i} : 2\gamma^{nl}(\Delta u_i, \delta u)) d\Omega \\ & 2\chi^p \Delta \chi_r + \sum_{i=1}^{r-1} \Delta \chi_i \Delta \chi_{r-i} = \frac{3}{2\sigma_y^2} \left(2S^{pd} : \Delta S_r^d + \sum_{i=1}^{r-1} \Delta S_i^d : \Delta S_{r-i}^d \right) \\ & r\chi^p \Delta \xi_r + \sum_{i=1}^{r-1} i \xi_i \chi_{r-i} = (n-1) \left(r \xi^p \Delta \chi_r + \sum_{i=1}^{r-1} i \Delta \xi_{r-i} \Delta \chi_i \right) \\ & \langle \Delta u_r, \Delta u' \rangle + \Delta \lambda_r \Delta \lambda' = 0 \end{aligned} \right. \quad (41)$$

Where $(\Delta u', \Delta \lambda')$ is the slope of the response curve and

$$\begin{aligned} \Delta S_r^{res} &= - \frac{1}{E(1 + \alpha \eta^n)} D_t : \left[\sum_{i=1}^{r-1} \Delta \xi_{r-i} \Delta S_i^d + \sum_{i=1}^{r-1} \left[\frac{3\xi^p (n-1)}{4\chi^{p2} \sigma_y^2} \Delta S_i^d : \Delta S_{r-i}^d - \frac{\xi^p (n-1)}{2\chi^{p2}} \Delta \chi_i \Delta \chi_{r-i} \right. \right. \\ & \left. \left. + \frac{i}{r\chi^p} \left((n-1) \Delta \chi_i \Delta \xi_{r-i} - \Delta \chi_{r-i} \Delta \xi_i \right) \right] S^{pd} \right] \end{aligned}$$